

## Supporting Information

### Highly flexible and stretchable MWCNT/HEPCP nanocomposites integrated near-IR, temperature and stress sensitivity for electronic skin

Mei Li, Yunming Wang\*, Yun Zhang, Huamin Zhou, Zhigao Huang, Dequn Li

#### Characterization of MWCNT/HEPCP nanocomposite films

Fourier transform infrared spectroscope (FTIR):

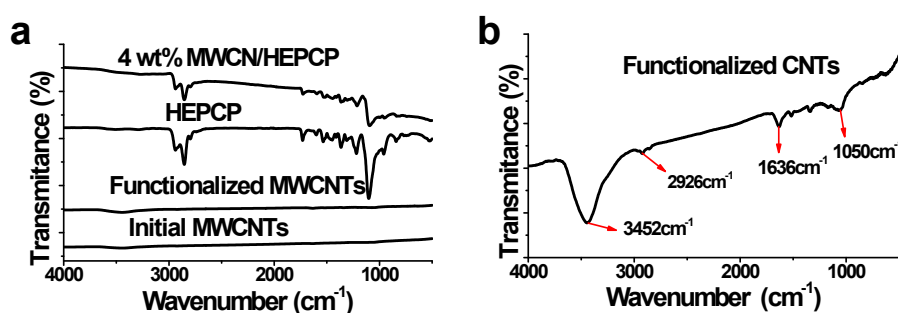


Fig. S1 The FTIR spectroscopic of initial MWCNTs, functionalized MWCNTs, HEPCP, 4 wt% MWCNT/HEPCP nanocomposite.

Functionalized MWCNTs (Fig. S1b): There is no infrared absorption peak between  $1700\text{ cm}^{-1}$  and  $3000\text{ cm}^{-1}$ .

HEPCP:  $2860\text{ (v CH}_2\text{) cm}^{-1}$ ,  $1732\text{ (v C=O) cm}^{-1}$ ,  $1533$  and  $1452\text{ (v C=C aromatic) cm}^{-1}$ ,  $1366\text{ (v}_{as}\text{ CH}_2\text{) cm}^{-1}$ ,  $1218\text{ (v}_{as}\text{ C-N aromatic) cm}^{-1}$ ,  $1100\text{ (v}_s\text{ CH}_2\text{) cm}^{-1}$ ,  $956\text{ (v}_{as}\text{ C-O-C) cm}^{-1}$ .

MWCNT/HEPCP nanocomposites:  $2860\text{ (v CH}_2\text{) cm}^{-1}$ ,  $1732\text{ (v C=O) cm}^{-1}$ ,  $1530$  and  $1448\text{ (v C=C aromatic) cm}^{-1}$ ,  $1366\text{ (v}_{as}\text{ CH}_2\text{) cm}^{-1}$ ,  $1213\text{ (v}_{as}\text{ C-N aromatic) cm}^{-1}$ ,  $1093\text{ (v}_s\text{ CH}_2\text{) cm}^{-1}$ ,  $952\text{ (v}_{as}\text{ C-O-C) cm}^{-1}$ .

#### UV-Vis-NIR spectroscope:

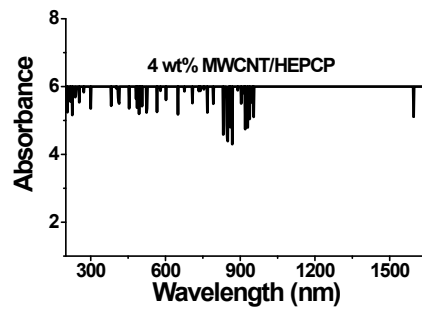


Fig. S2 The UV-vis-NIR spectroscope of 4 wt% MWCNT/HEPCP nanocomposite film (Thickness, 0.4 mm).

#### Sensitivity to IR illumination, temperature, and tensile strain

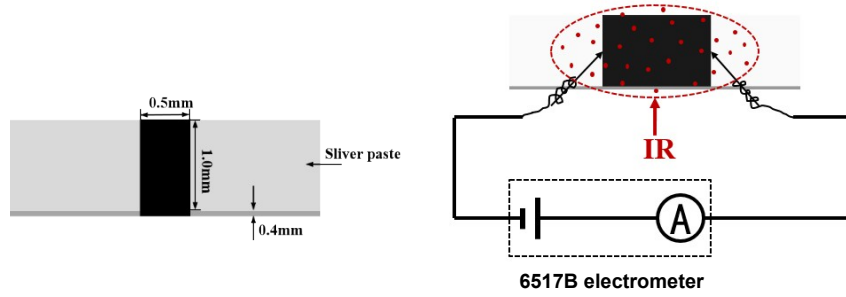


Fig. S3 The schematic diagram of the IR response test experiments (sample size:  $1.0\text{ mm} \times 0.5\text{ mm} \times 0.4\text{ mm}$ ).

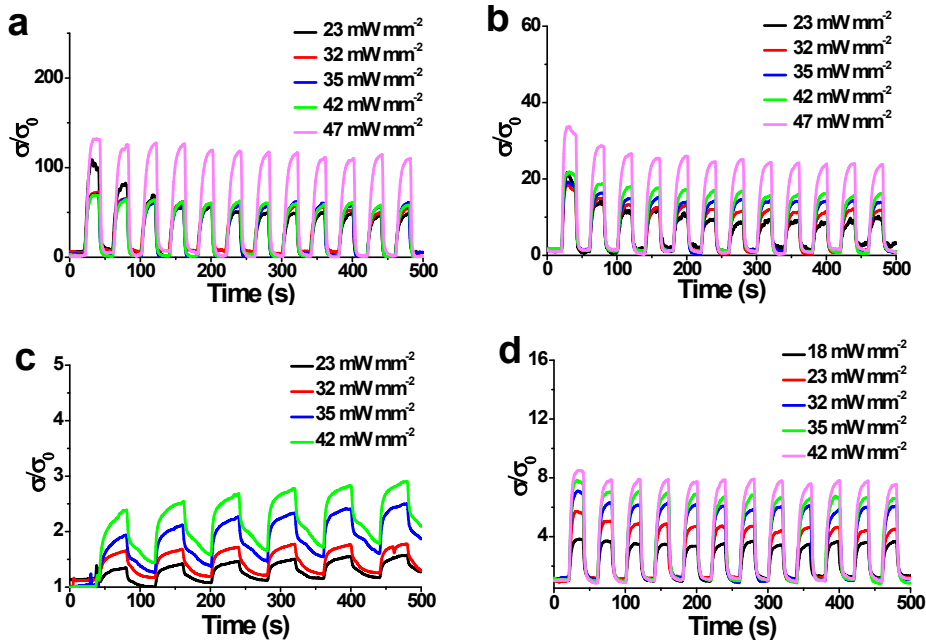


Fig. S4 The IR-regulated on/off electrical conductivity ratio of the MWCNT/HEPCP nanocomposite films at different IR power density (IR power density: 18, 23, 32, 35, 42 and  $47\text{ mW mm}^{-2}$ ): (a) 3 wt% MWCNT/HEPCP nanocomposite; (b) 5 wt% MWCNT/HEPCP nanocomposite; (c) 7 wt% MWCNT/HEPCP nanocomposite; (d) 8 wt% MWCNT/HEPCP nanocomposite.

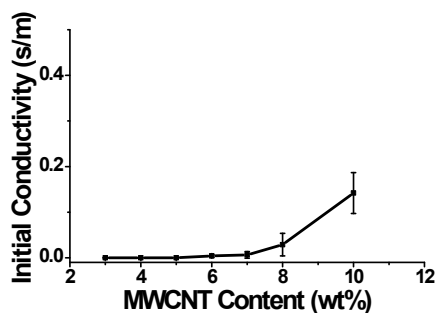


Fig. S5 Initial electrical conductivity of MWCNT/HEPCP nanocomposite films (3 wt%–10 wt%; sample size:  $1.0\text{ mm} \times 0.5\text{ mm} \times 0.4\text{ mm}$ ) measured at room temperature before IR, temperature and tensile strain response test.

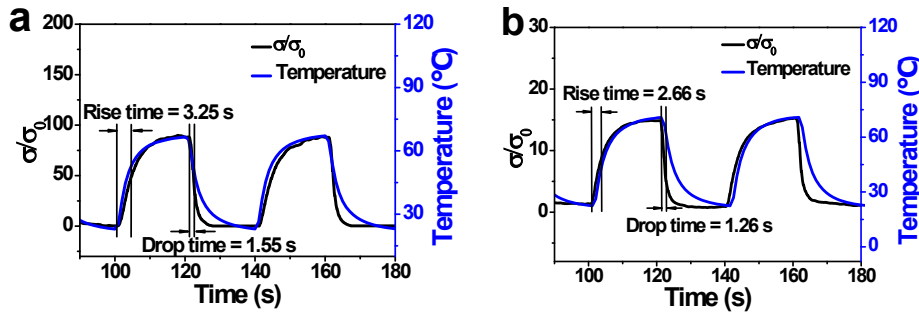


Fig. S6 The response time of IR and temperature profiles for (a) the 3 wt% and (b) 5 wt% MWCNT/HEPCP nanocomposites at an IR power density of 35 mW mm $^{-2}$ .

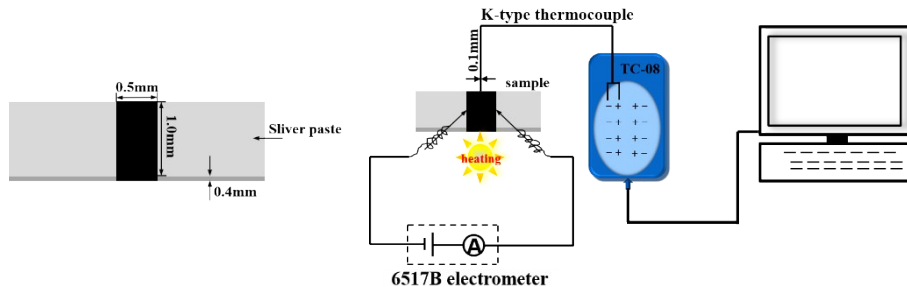


Fig. S7 The sample size and experimental schematic of the temperature response test (sample size: 1.0 mm  $\times$  0.5 mm  $\times$  0.4 mm).

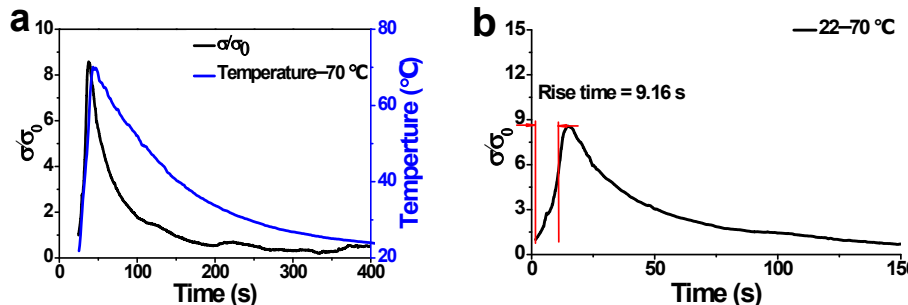


Fig. S8 (a) The temperature dependence electrical conductivity ratio ( $\sigma/\sigma_0$ ) and temperature profile correspond to the heating process from room temperature to 70  $^{\circ}\text{C}$  in 20 s, then cooling to the room temperature at room temperature. (b) The response time (the time taken for the conductivity rise to 63.2% of the total magnitude of conductivity change during heating.) of temperature dependence electrical conductivity ratio ( $\sigma/\sigma_0$ ) of 4 wt% MWCNT/HEPCP during the heating process from room temperature to 70  $^{\circ}\text{C}$  in 20 s.

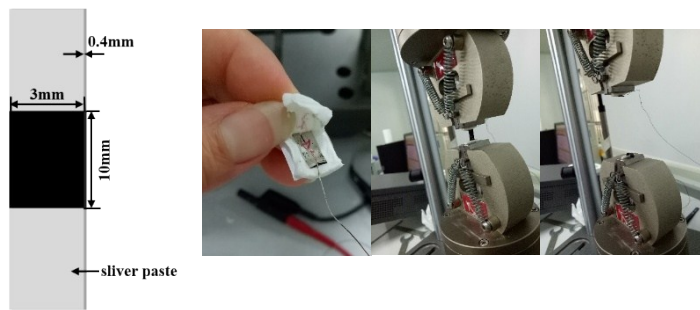


Fig. S9 The sample size and experiment device diagram of the tensile stress response test (sample size: 10 mm  $\times$  3 mm  $\times$  0.4 mm).

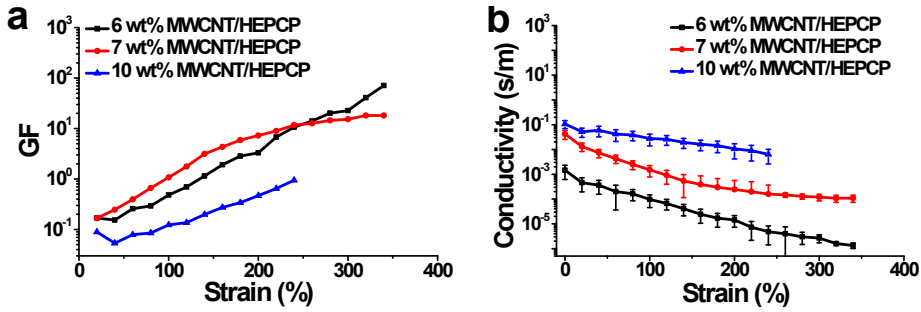


Fig. S10 (a) Gauge factor of the 6, 7 and 10 wt% MWCNT/HEPCP nanocomposite films as a function of tensile strain; (b) Electrical conductivity of 6, 7 and 10 wt% MWCNT/HEPCP nanocomposite films as a function of tensile strain.

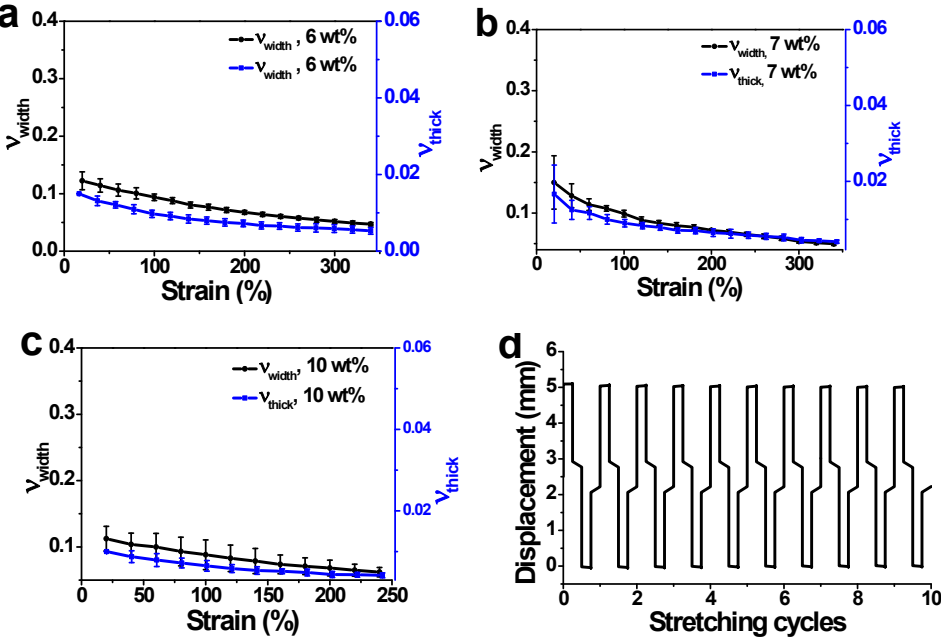


Fig. S11 Poisson's ratio of width and thickness of (a) 6 wt%, (b) 7 wt% and (c) 10 wt% MWCNT/HEPCP nanocomposite films as a function of tensile strain; (d) The displacement of 6 wt% MWCNT/HEPCP nanocomposite film in the recurrent stretching cycles, strain  $\epsilon = 50\%$ .

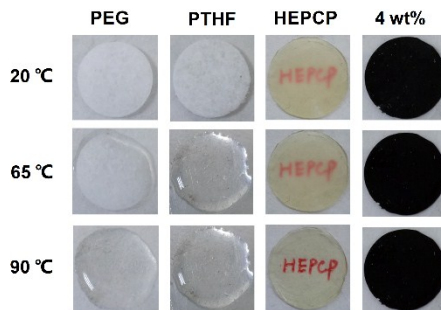


Fig. S12 Comparison of the macroscopic morphology of the pure PEG (6 kDa), pure PTHF (2.9 kDa), HEPCP and 4 wt% MWCNT/HEPCP nanocomposite at different temperatures.

### Mechanism underlying the IR, temperature, and tensile stress response of the nanocomposites

Differential Scanning Calorimetry (DSC):

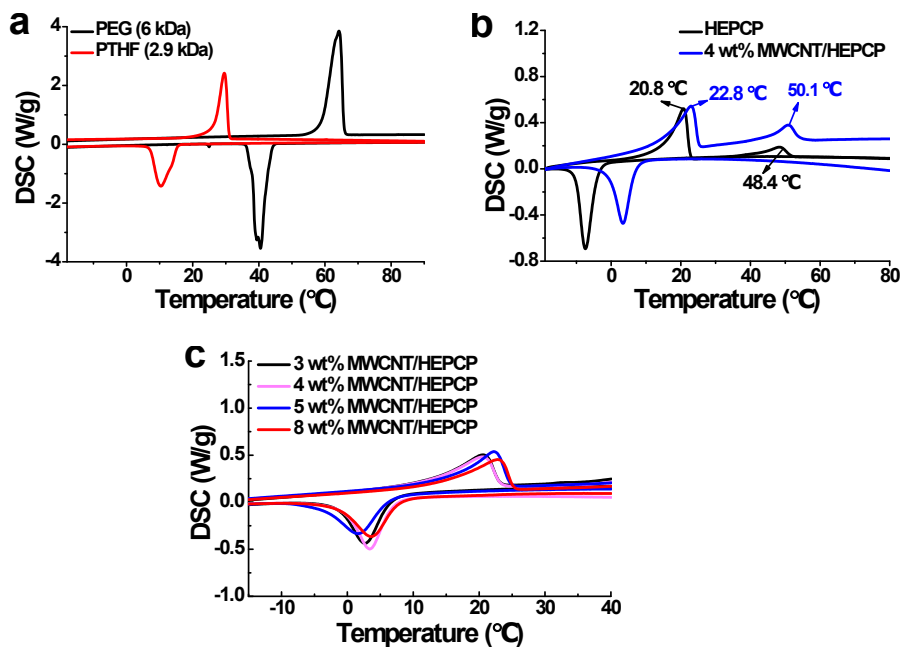


Fig. S13 The DSC curve of PEG (6 kDa), PTHF (2.9 kDa), HEPCP and MWCNT/HEPCP nanocomposites (heating and cooling rate:  $5\text{ }^{\circ}\text{C min}^{-1}$ ): (a) The DSC curve of PEG (6 kDa), PTHF (2.9 kDa); (c) The DSC curve of HEPCP and 4 wt% MWCNT/HEPCP nanocomposite; (b) The DSC curve of 3 wt%, 4 wt%, 5 wt% and 8 wt% MWCNT/HEPCP nanocomposites.

Table S1 Phase transition behavior of PEG (6 kDa), PTHF (2.9 kDa), HEPCP and MWCNT/HEPCP nanocomposites.

Sample	$\Delta H [\text{J g}^{-1}]$		$T_m [\text{ }^{\circ}\text{C}]$	$T_c [\text{ }^{\circ}\text{C}]$
	Heatin	Cooling	Heating	Cooling
PEG [6 kDa]	173.88	167.34	64.21	40.50
PTHF [2.9 kDa]	95.06	88.08	39.38	10.45
HEPCP	37.65	36.43	20.77	-7.42
3 wt%	30.50	31.81	22.75	2.75
4 wt%	37.69	33.73	22.75	3.42
5 wt%	31.53	34.28	22.25	1.77
7 wt%	45.09	36.56	24.33	5.24
8 wt%	32.98	31.75	22.75	3.58

(Where  $\Delta H$  is the enthalpy of the phase transition;  $T_m$  is the melting peak temperature;  $T_c$  is the recrystallization peak temperature.)